AMERICAN SOCIETY FOR MICROBIOLOGY | Antimicrobial Agents and Chemotherapy

# *Nicotiana alata* Defensin Chimeras Reveal Differences in the Mechanism of Fungal and Tumor Cell Killing and an Enhanced Antifungal Variant

**Mark R. Bleackley,[a] Jennifer A. E. Payne,[a] Brigitte M. E. Hayes,[a] Thomas Durek,[b] David J. Craik,[b] Thomas M. A. Shafee,[a] Ivan K. H. Poon,[a] Mark D. Hulett,[a] Nicole L. van der Weerden,[a] Marilyn A. Anderson[a]**

Department of Biochemistry and Genetics, La Trobe Institute for Molecular Science, La Trobe University, Melbourne, Victoria, Australia[a]; Institute for Molecular Bioscience, The University of Queensland, Brisbane, Queensland, Australia[b]

**The plant defensin NaD1 is a potent antifungal molecule that also targets tumor cells with a high efficiency. We examined the features of NaD1 that contribute to these two activities by producing a series of chimeras with NaD2, a defensin that has relatively poor activity against fungi and no activity against tumor cells. All plant defensins have a common tertiary structure known as a cysteine-stabilized α-β motif which consists of an α helix and a triple-stranded β-sheet stabilized by four disulfide bonds. The chimeras were produced by replacing loops 1 to 7, the sequences between each of the conserved cysteine residues on NaD1, with the corresponding loops from NaD2. The loop 5 swap replaced the sequence motif (SKILRR) that mediates tight binding with phosphatidylinositol 4,5-bisphosphate [$PI(4,5)P_2$] and is essential for the potent cytotoxic effect of NaD1 on tumor cells. Consistent with previous reports, there was a strong correlation between $PI(4,5)P_2$ binding and the tumor cell killing activity of all of the chimeras. However, this correlation did not extend to antifungal activity. Some of the loop swap chimeras were efficient antifungal molecules, even though they bound poorly to $PI(4,5)P_2$, suggesting that additional mechanisms operate against fungal cells. Unexpectedly, the loop 1B swap chimera was 10 times more active than NaD1 against filamentous fungi. This led to the conclusion that defensin loops have evolved as modular components that combine to make antifungal molecules with variable mechanisms of action and that artificial combinations of loops can increase antifungal activity compared to that of the natural variants.**

Innate immunity peptides have evolved in plants to protect against the damaging effects of microbial pathogens, particularly fungi (1). Fungi cause both persistent annual crop losses and devastating epidemics (2) that are a serious threat to global food security (3). Plants lack the adaptive immune system of mammals and instead rely on a suite of antifungal peptides to ward off infection (1). Defensins are a major family of plant antifungal peptides (4, 5), and some members have been studied extensively because of their potential use in transgenic plants for protection against fungal disease (6–8).

Plant defensins are small peptides (45 to 54 amino acids) that are basic and cysteine rich. They have a conserved three-dimensional structure composed of three β-strands linked to an α-helix by three disulfide bonds together with a fourth disulfide bond that links the N- and C-terminal regions and creates a pseudo cyclic structure (9). Beyond the 8 cysteine residues and a conserved glycine that is required for the structural fold, there is a great deal of sequence variability across the plant defensin family. This variability is displayed in seven loops (loop 1 [L1] to L7) that correspond to the regions between cysteine residues (Fig. 1) (5). The sequence diversity explains the wide range of functions that have been reported for plant defensins, including antibacterial and antifungal activities as well as roles in plant development, sexual reproduction, and metal tolerance (reviewed in reference 5). Some antifungal defensins display activity against tumor cells but not healthy mammalian cells (10, 11). However, it remains to be established if the mechanism of action against fungal and mammalian tumor cells is the same.

Fungal cell killing by the defensin NaD1 from the ornamental tobacco *Nicotiana alata* occurs through a mechanism that involves specific interaction with the fungal cell wall before it passes through the plasma membrane and enters the fungal cytoplasm. Once inside the cell, NaD1 rapidly initiates the production of reactive oxygen species (ROS), permeabilization of the fungal plasma membrane, and cell death (12–14). The activity against tumor cell lines is mediated by a specific and high-affinity interaction with phosphatidylinositol 4,5-bisphosphate [$PI(4,5)P_2$]. This lipid binding specificity has been described only for the class II defensins from the Solanaceae among plant defensins and is largely mediated through the sequence in loop 5 (10, 11, 15). Class II defensins have a C-terminal propeptide that directs them to the vacuole, whereas class I defensins lack this sequence and are secreted by default from the plant cell (9). Interestingly, even though human and plant defensins have evolved separately (16), a related sequence in loop 5 of human β-defensin 3 (17) is required for

**Received** 7 July 2016 **Returned for modification** 22 July 2016
**Accepted** 3 August 2016
**Accepted manuscript posted online** 8 August 2016
**Citation** Bleackley MR, Payne JAE, Hayes BME, Durek T, Craik DJ, Shafee TMA, Poon IKH, Hulett MD, van der Weerden NL, Anderson MA. 2016. *Nicotiana alata* defensin chimeras reveal differences in the mechanism of fungal and tumor cell killing and an enhanced antifungal variant. Antimicrob Agents Chemother 60:6302–6312. doi:10.1128/AAC.01479-16.

Address correspondence to Mark R. Bleackley, m.bleackley@latrobe.edu.au, or Marilyn A. Anderson, m.anderson@latrobe.edu.au.

M.R.B. and J.A.E.P. contributed equally to this article, and N.L.V.D.W. and M.A.A. contributed equally to this article.

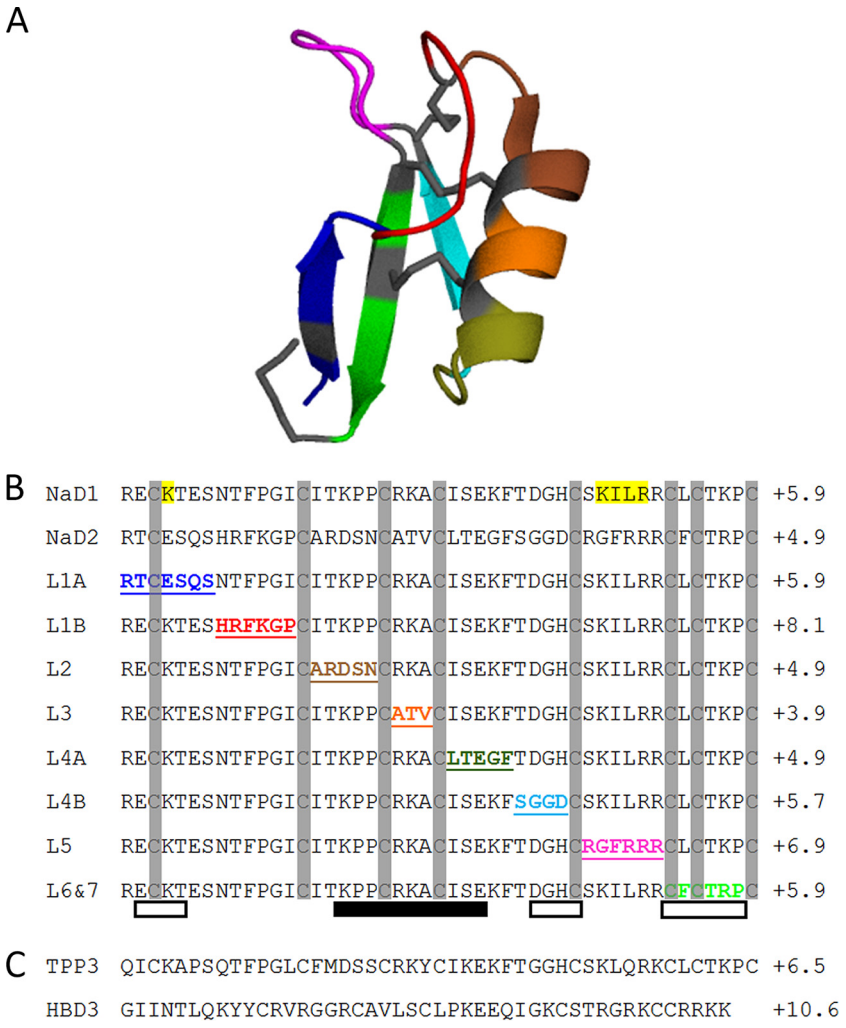


**FIG 1** Loop swap variants of NaD1 and NaD2. (A) Loops are defined as intercysteine sequences (shown here using NaD1 as a model with cysteine residues and disulfides in gray). The residues that participate in the interaction between NaD1 and PI(4,5)$P_2$ are highlighted in yellow in the NaD1 sequence. L1A (blue) consists of the first β-strand. L1B (red) is the random-coil/turn region joining the strand to the α-helix. L2 (brown), L3 (yellow), and L4A (olive) make up the α-helix. L4B (cyan) forms the second β-strand. L5 (pink) is a surface loop connecting two β-strands, and L6 and L7 (L6&7; green) form the final β-strand (PDB accession number 4AAZ [26]). (B) Sequence alignment of the loop-swapped proteins, which contain a loop of NaD2 in the NaD1 framework. The NaD2 loop sequences are color coded as described in the legend to panel A. The column on the right indicates the charge of each defensin at pH 7. The white boxes below the sequences indicate regions that form β-strands, and the black box indicates the helical region of NaD1. (C) Sequence and charge at pH 7 of two other proteins reported to bind PI(4,5)P, TPP3 and HBD3.

PI(4,5)$P_2$ binding and tumor cell killing. The defensins NaD1 and TPP3 from tomatoes both dimerize and form the cationic grip which binds two PI(4,5)$P_2$ molecules. The defensin-PI(4,5)$P_2$ dimer then forms oligomers via a different interface (10). The interaction of NaD1 and TPP3 with PI(4,5)$P_2$ is proposed to lead to the characteristic blebbing and membrane permeabilization that occurs when tumor cells are treated with these defensins (10, 11). Indeed, masking of PI(4,5)$P_2$ by intracellular expression of a pleckstrin homology domain or treatment with neomycin delayed tumor cell killing by NaD1, supporting the role for PI(4,5)$P_2$ binding in the activity against tumor cells (10, 11). Mutations in residues that participate in PI(4,5)$P_2$ binding reduced both tumor and fungal cell killing by these defensins (10, 11).

NaD2 is another defensin produced by *N. alata* that has weaker antifungal activity than NaD1 against filamentous fungi and rusts (18). NaD2 is not a member of the solanaceous class II defensin family but is a member of the much larger family of class I defensins which are produced by all plant families. Here we report that unlike NaD1, NaD2 has no activity against tumor cells. We investigated the role of various sequence components in the lipid binding, tumor cell killing, and antifungal activities of NaD1 by swapping the loop regions of NaD1 for corresponding loops from NaD2. These studies revealed a strong correlation between PI(4,5)$P_2$ binding and tumor cell killing across all of the chimeric defensins. This correlation did not extend to the antifungal activities of the loop swap chimeras, indicating that the role of PI(4,5)$P_2$ binding is not as crucial in fungal cell killing by these defensins.

## MATERIALS AND METHODS

**Strains and vectors.** The *Fusarium oxysporum* f. sp. *vasinfectum* strain used in this study was an Australian isolate from cotton (Farming Systems

Institute, Department of Primary Industries, Queensland, Australia; a gift from Wayne O'Neill). *Aspergillus niger* (strain 5181), *Aspergillus flavus* (strain 5310), and *Aspergillus parasiticus* (strain 4467) spores (a gift from Dee Carter, University of Sydney) were grown on half-strength potato dextrose agar (PDA) plates. *Candida albicans* (strain DAY185) and *Cryptococcus neoformans* (strain H99; a gift from Dee Carter, University of Sydney) were grown on 1% yeast extract, 2% peptone, 2% dextrose (YPD) agar plates and cultured at 30°C in YPD. All experiments with *S. cerevisiae* were performed in a strain BY4741 (MAT**a** *his3Δ0 leu2Δ0 met15Δ0 ura3Δ0*) or BY4743 (*MAT***a**/α *his3Δ1/his3Δ1 leu2Δ0/leu2Δ0 LYS2/lys2Δ0 met15Δ0/MET15 ura3Δ0/ura3Δ0*) background. Deletion strains were retrieved from the nonessential knockout (*inp51*Δ, *inp52*Δ, *lsb6*Δ) or heterozygous essential knockout (*STT4/stt4*Δ, *PIK1/pik1*Δ, *MSS4/mss4*Δ) collection (Thermo Scientific). Native NaD1 and NaD2 were purified from *Nicotiana alata* flowers as described in reference 12. LL37 was purchased from GenScript (Hong Kong).

**Cloning and expression of loop swap proteins.** Loops in the NaD1 (GenBank accession no. Q8GTM0) defensin were replaced by the corresponding loops from NaD2 (GenBank accession no. KX688721) using Phusion mutagenesis (New England BioLabs) of an NaD1 construct in the pHUE expression vector (19). Both loops 1 and 4 were split into two shorter regions yielding an A and a B chimera for each loop. Loops 6 and 7 were both short and were thus combined when the chimeric proteins were made. Proteins were expressed in *Escherichia coli* T7 (New England BioLabs) according to the manufacturer's instructions and were purified using nickel affinity chromatography. The ubiquitin/His tag was removed using ubiquitin-specific protease 2 at a final concentration of 70 μg/ml, followed by reverse nickel affinity chromatography. Proteins were purified further by reverse-phase high-performance liquid chromatography using a Zorbax $C_8$ analytical column (Agilent). Correct folding of loop swap variants was confirmed by circular dichroism (CD).

**Circular dichroism.** Stock solutions of each of the proteins were prepared in $H_2O$ (~0.5 to 1.0 mg/ml) and diluted 1:4 in 10 mM sodium phosphate buffer, pH 6.8, prior to measurement. CD spectra at wavelengths ranging from 185 to 260 nm were recorded on a Jasco J-810 spectropolarimeter at room temperature using quartz cuvettes with a path length of 1 cm (151 data points per scan; bandwidth, 1.7 nm; response, 1 s; scan speed, 100 nm/min). The value for the buffer blank was subtracted, and the spectra were smoothed using the algorithm included in the Jasco data analysis software and plotted using GraphPad Prism software. Fractional helicity ($f_H$) was calculated as described in reference 20.

**Antifungal assays.** Antifungal assays were performed with *F. oxysporum*, *Fusarium graminearum*, and *Colletotrichum graminicola* as described in reference 12. *F. oxysporum* and *F. graminearum* growth was assayed after 24 h, and *C. graminicola* growth was assayed after 48 h. Assays with *C. albicans*, *C. neoformans*, and *S. cerevisiae* were performed as described in reference 21. The 50% inhibitory concentrations ($IC_{50}$s) for *F. oxysporum* were identified from the growth inhibition curves. The 95% confidence intervals (CIs) were calculated. Overlapping CIs were assigned the same letter, and values with different letters were significantly different.

**Tumor cell permeabilization assays.** Permeabilization of cells from a human monocytic lymphoma cell line, U937, was monitored using a propidium iodide (PI) uptake assay as described in reference 10 with some modifications. Protein at 0, 2.5, 5, 10, or 20 μM was incubated with $4 \times 10^4$ cells in RPMI 1640 medium (Thermo) containing 0.1% bovine serum albumin (Sigma-Aldrich) for 30 min at 37°C, before the addition of PI (Sigma-Aldrich) to a final concentration of 1 μg/ml. Samples were placed on ice and analyzed by flow cytometry using a FACSCanto II flow cytometer with FACSDiva software (v6.1.1; BD Biosciences). Data were analyzed by FlowJo software (Tree star) by gating cells on the basis of forward and side scatter. Cell permeabilization was defined by PI fluorescence. Statistical analysis was performed as described above for the antifungal assays.

**Permeabilization of liposomes.** Liposomes were prepared as outlined in reference 10. Permeabilization of liposomes was assessed by monitoring the release of entrapped calcein as described in references 22 and 13. The fluorescence of the released calcein was used as a measure of permeabilization and was calculated relative to that of the Triton X-100 (0.1%)-treated positive control. Statistical analysis was performed as described above for the antifungal assays.

**Fungal membrane permeabilization assays.** Membrane permeabilization was monitored using SYTOX green as outlined in reference 13. Assays for the permeabilization activity of loop swap variants against *F. oxysporum* hyphae were performed using test proteins at 10 μM.

**Lipid binding.** Binding of protein to a variety of membrane lipids was tested using PIP strips (batch numbers KE071312 and KE020212; Echelon Biosciences, Salt Lake City, UT), as described in the manufacturer's protocol and in reference 10. Antibodies to NaD1 and NaD2 were polyclonal antibodies developed in rabbits.

**Yeast survival assays.** *S. cerevisiae* BY4741 cells were grown overnight at 30°C in YPD. Aliquots of an overnight culture (500 μl) were treated with neomycin (10, 1, 0.1, 0 mM) for 3 h. Cells were washed three times with half-strength potato dextrose broth (1/2 PDB; BD Difco) and then diluted in 1/2 PDB to an optical density at 600 nm of 0.2. Cells were treated with 20 and 10 μM NaD1, 30 and 15 μM LL37, 50 and 25 μM L5, and water for 1 h at 30°C with shaking. To determine the survival of yeast cells in each treatment, a 5-fold dilution series of each treatment combination was plated on YPD agar plates and incubated at 30°C for 2 days. Images of the plates were taken using a ChemiDoc imager (Bio-Rad) at the epi-White settings. Data were consistent across three independent biological experiments.

**Accession number.** NaD2 has been deposited in GenBank under accession no. KX688721.

## RESULTS

**Protein expression and folding.** Eight NaD1-NaD2 loop swap proteins were produced recombinantly in *E. coli* using the pHUE expression system. These proteins consisted of an NaD1 backbone in which each of the loops of NaD1 was replaced with the corresponding loop from NaD2 (Fig. 1). Purified recombinant protein was analyzed by SDS-PAGE and matrix-assisted laser desorption ionization mass spectrometry to ensure that the expressed proteins were of the expected size (data not shown). Two of the recombinant proteins, L2 and L3, did not express well and were not included in subsequent experiments. Loops 1 and 4 are the longer loops in plant defensins and as such were each split across two chimeric defensins, denoted A and B. Loops 6 and 7 are the shortest loops in plant defensins (1 and 3 amino acids, respectively) and were thus combined into a single chimeric defensin. L1A was expressed at very low levels and was omitted from some experiments. The CD spectra of recombinantly expressed NaD1 and NaD2 were similar to those of NaD1 and NaD2 purified from plants, demonstrating that the recombinant expression system produced defensins with the correct fold (Fig. 2A). On the basis of the mean residue ellipticity at 222 nm ($[\Theta]_{222}$), the helical content (represented as the fractional helicity [$f_H$]) for NaD1 and NaD2 was ~16% and ~6%, respectively (Fig. 2C). The CD-estimated value for NaD1 was slightly lower than the actual helical content (~23%) in the nuclear magnetic resonance and X-ray structures but consistent with it, considering that the CD data provide only broad estimates. The CD spectra of all the loop swap proteins were similar to the NaD1 spectrum, with $f_H$ values generally being in the range of 16 to 18% (Fig. 2B). The largest differences were for the CD spectra of L4A, with an $f_H$ value of 24%, and L6-L7, with an $f_H$ value of 12%. L4A locates to the C-terminal cap region of the single α-helix in the cysteine-stabilized αβ motif structure of NaD1, and hence, changes in this region can be expected to directly affect helix propensity. Loop swaps with L6-L7 are ex-

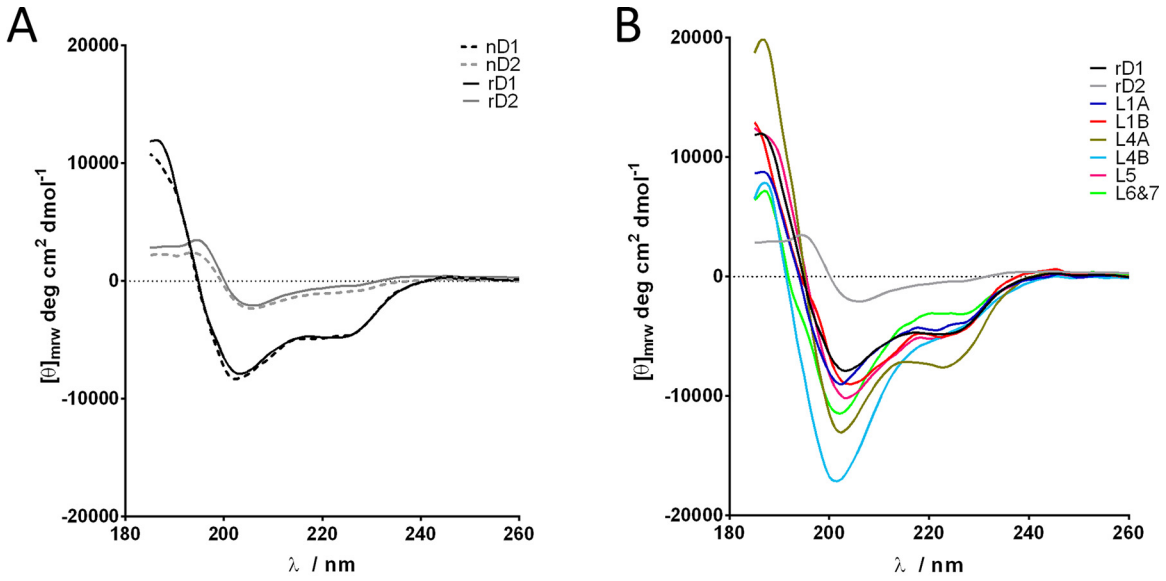


C

| Peptide | $[\theta]_{222}$ (MRW) | $F_{helix}$/% |
|---|---|---|
| rNaD1 | -4813 | 16.5 |
| nNaD1 | -4742 | 13.2 |
| rNaD2 | -502 | 4.8 |
| nNaD2 | -1025 | 6.2 |
| L1A | -4460 | 15.6 |
| L1B | -5059 | 17.2 |
| L4A | -7580 | 24.0 |
| L4B | -5144 | 17.4 |
| L5 | -5174 | 17.5 |
| L6&7 | -3123 | 11.9 |

**FIG 2** Circular dichroism of purified loop swap variants. (A) Recombinantly expressed and purified defensins (recombinant NaD1 and NaD2 [rD1 and rD2, respectively]) have the same CD spectra as those purified from plants (natural NaD1 and NaD2 [nD1 and nD2, respectively]), indicating that the secondary structure elements formed correctly. (B) Loop swap variants have CD spectra similar to those of the native sequences, demonstrating correct folding of the proteins.(C) Percent helicity of native and recombinant NaD1 (rNaD1), recombinant NaD2 (rNaD2), and the loop swap variants. nNaD1 and nNaD2, natural NaD1 and NaD2, respectively; MRW, mean residue weight; $F_{helix}$, fractional helicity.

pected to affect the C-terminal β-strand. Despite the relatively conservative substitutions (CLCTKPC in NaD1 versus CFC TRPC in L6-L7), the helix propensity may have been impacted indirectly because the α-helix and C-terminal β-strand are tethered via two disulfide bonds (Fig. 1). L4B had a deeper trough at 200 nm, indicating an increase in random coil secondary structure. Loop 4B forms one of the β-strands, and modification of this sequence may have affected formation of the secondary structure.

**Antifungal activity of NaD1-NaD2 loop swap chimeras against *F. oxysporum*.** The antifungal activity of the native floral defensins and the recombinantly expressed defensins against *F. oxysporum* was assessed. NaD1 ($IC_{50}$, 1.5 ± 0.25 μM) was more active than NaD2 ($IC_{50}$, 8.3 ± 2.1 μM) (Fig. 3A and D). The $IC_{50}$s of recombinant NaD1 and NaD2 did not differ significantly from those of the proteins isolated from plants, demonstrating that recombinant expression had no effect on the activity of these defensins (data not shown). Swapping the L4A or L4B sequences of NaD2 into the NaD1 backbone had no effect on the antifungal activity of the defensin. However, replacement of L1A and L5 of NaD1 with the corresponding NaD2 sequence decreased the activity of the chimeric defensins. Increased activity was observed when either L1B or L6-L7 of NaD2 was inserted into the NaD1 framework in place of the native sequence. The loop 1B swap produced the most active variant, which had an $IC_{50}$ of 0.2 ± 0.04 μM; in comparison, the $IC_{50}$s were 1.5 ± 0.3 μM for NaD1 and 8.3 ± 2.1 μM for NaD2. The least active variant was L1A, which had an $IC_{50}$ of 3.2 ± 0.8 μM (Fig. 3A and D).

**Activity against a model tumor cell line.** Tumor cell killing by native and recombinant defensins was determined by monitoring propidium iodide (PI) uptake into the model monocytic lymphoma cell line U937. Recombinant NaD1 was much more efficient at permeabilizing and killing U937 cells than recombinant NaD2 (Fig. 3B). Replacement of either loop 4A or loops 6 and 7 of NaD1 with the corresponding loops from NaD2 had no effect on the tumor cell killing activity compared to that of NaD1. However, substitution of loop 1A, 1B, 4B, or 5 generated chimeric defensins with less antitumor cell activity than NaD1 (Fig. 3B and D). None of the loop swap variants had increased activity relative to that of NaD1 against U937 cells.

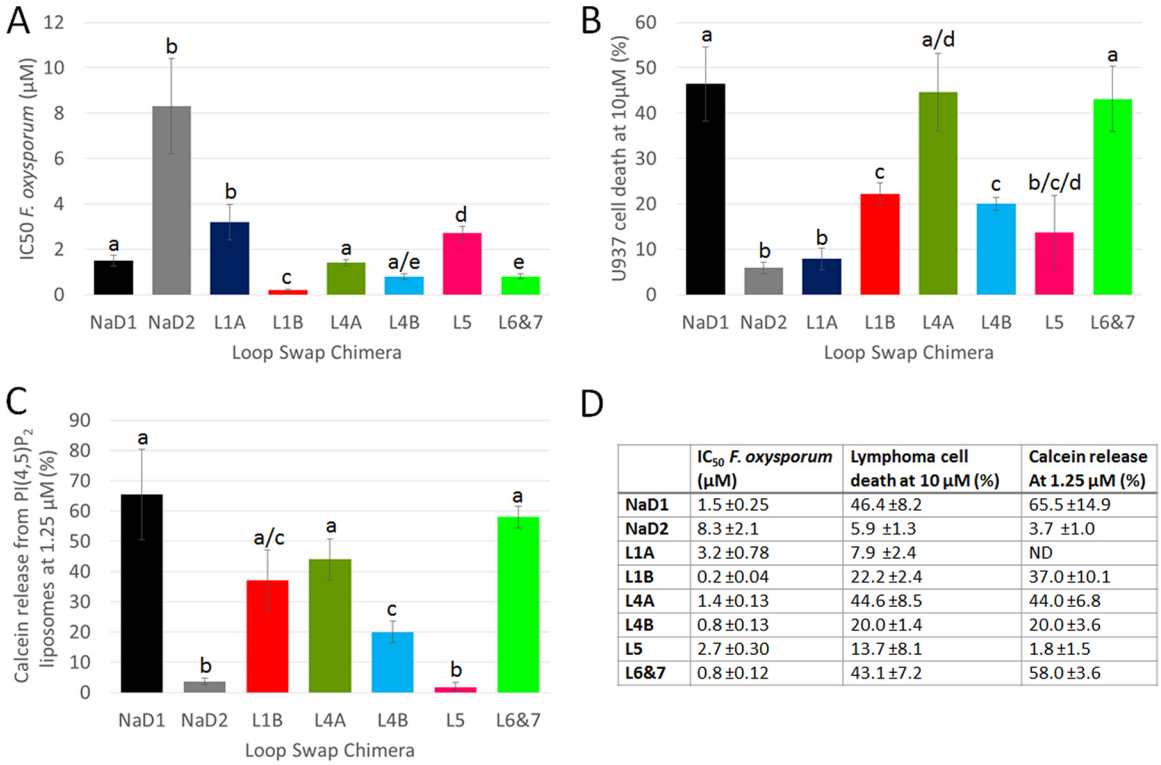


D

| | $IC_{50}$ *F. oxysporum* (μM) | Lymphoma cell death at 10 μM (%) | Calcein release At 1.25 μM (%) |
|---|---|---|---|
| **NaD1** | 1.5 ±0.25 | 46.4 ±8.2 | 65.5 ±14.9 |
| **NaD2** | 8.3 ±2.1 | 5.9 ±1.3 | 3.7 ±1.0 |
| **L1A** | 3.2 ±0.78 | 7.9 ±2.4 | ND |
| **L1B** | 0.2 ±0.04 | 22.2 ±2.4 | 37.0 ±10.1 |
| **L4A** | 1.4 ±0.13 | 44.6 ±8.5 | 44.0 ±6.8 |
| **L4B** | 0.8 ±0.13 | 20.0 ±1.4 | 20.0 ±3.6 |
| **L5** | 2.7 ±0.30 | 13.7 ±8.1 | 1.8 ±1.5 |
| **L6&7** | 0.8 ±0.12 | 43.1 ±7.2 | 58.0 ±3.6 |

**FIG 3** The antifungal, antitumor, and liposome-permeabilizing activities of the NaD1-NaD2 loop swap proteins. (A) The concentration of the NaD1-NaD2 loop swap proteins required to inhibit the growth of the filamentous fungus *F. oxysporum* by 50% ($IC_{50}$). The loop swap proteins L4B, L6-L7, and, particularly, L1B had enhanced antifungal activity relative to that of NaD1, whereas L1A and L5 had decreased activity. (B) Activity of the NaD1-NaD2 loop swap proteins against the U937 lymphoma cell line. Cell death was assessed by determination of the level of PI uptake into cells by flow cytometry after treatment with test protein at 10 μM. All of the loop swap proteins, apart from L4A, L6, and L7, had less activity than recombinant NaD1. (C) The release of calcein from PC-PE-PS-PI-$PI(4,5)P_2$ liposomes by loop swap chimeras (1.25 μM) after 10 min relative to that of the Triton X-100-treated control. NaD1 readily permeabilized liposomes, while NaD2 had minimal permeabilization activity. All of the loop swap chimeras permeabilized liposomes with activities intermediate to those of NaD1 and NaD2, except for L5, which did not permeabilize liposomes at all. Error bars are means ± SEMs ($n = 3$). Letters above the bars indicate overlapping 95% confidence intervals. Values with the same letter are not significantly different.

**Permeabilization of $PI(4,5)P_2$ liposomes.** A calcein release assay was used to determine the permeabilizing activity of the native defensins and the loop swap variants on bilayers of defined composition. Phosphatidylcholine (PC)-phosphatidyl (PE)-phosphatidylserine (PS)-phosphatidylinositol (PI) liposomes (molar ratio, 52:30:10:8) were prepared with and without $PI(4,5)P_2$ (4%) and were loaded with calcein prior to incubation with each of the defensins (1.25 μM) for 10 min. Liposomes without $PI(4,5)P_2$ were not permeabilized at a significant level by any of the defensins tested (data not shown). When $PI(4,5)P_2$ was present, NaD1 treatment released the most calcein, whereas NaD2 had no activity (Fig. 3C and D). There was no significant difference in permeabilization of the $PI(4,5)P_2$ liposomes by the L1B, L4A, and L6-L7 chimeras from that of NaD1. In contrast, the L4B chimera had significantly less permeabilization activity than NaD1, and the L5 chimera had none.

**Permeabilization of the *F. oxysporum* plasma membrane by loop swap chimeras.** Permeabilization of the *F. oxysporum* plasma membrane was assayed by monitoring the uptake and fluorescence of the non-membrane-permeant dye SYTOX green over a period of 180 min (Fig. 4). After a 20-min delay, there was a steady increase in the fluorescence of the NaD1 (10 μM)-treated hyphae for the following 80 min. Hyphae incubated with 10 μM NaD2 showed no increase in fluorescence over the 180-min time period, indicating that this defensin did not permeabilize the plasma membrane. The loop 5 chimera displayed permeabilization kinetics similar to those of NaD1. All the other loop swap chimeras had permeabilization profiles intermediate between those of NaD1 and NaD2. L1A permeabilized more slowly than

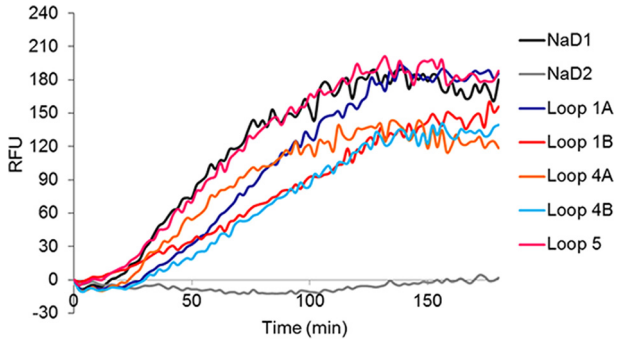


**FIG 4** Permeabilization of *F. oxysporum* hyphae by NaD1-NaD2 loop swap variants. Permeabilization of *F. oxysporum* was assessed by monitoring the uptake and fluorescence of the non-cell-permeant dye SYTOX green. All of the loop swap variants permeabilized hyphae but did so to variable extents. NaD2 did not permeabilize hyphae at all. L5 displayed permeabilization kinetics similar to those of NaD1, while the remaining loop swap variants all had lower rates of permeabilization than NaD1. Data are representative of those from three independent assays. RFU, relative fluorescence units.

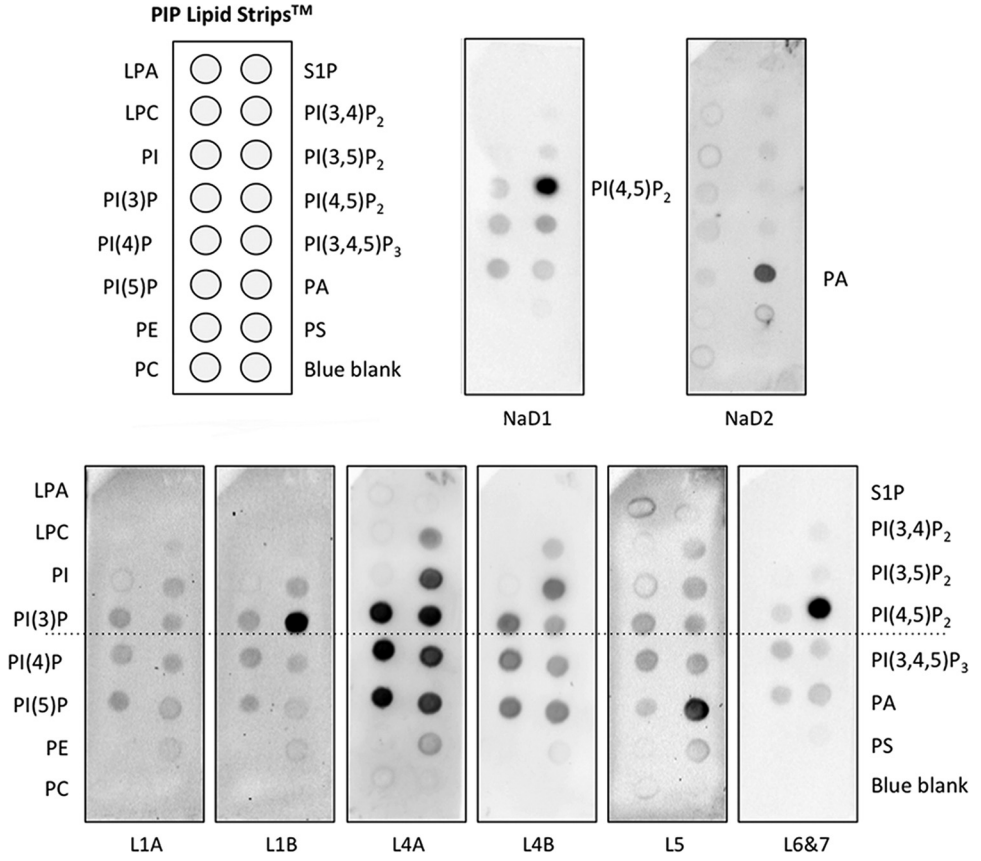


**FIG 5** Lipid strip binding profiles of NaD1, NaD2, and the loop swap chimeras. The introduction of the different loop regions from NaD2 into NaD1 changed the lipid binding profiles of the protein. Binding of NaD1 and the loop-swapped proteins to PIP strips was detected by Western blotting with polyclonal rabbit anti-NaD1 IgG, while NaD2 binding was detected with polyclonal rabbit anti-NaD2 IgG. Images are representative of those from two separate experiments with different batches of strips. LPA, lysophosphatidic acid; LPC, lysophosphocholine; PI, phosphatidylinositol; pPI(3)P, phosphatidylinositol 3-phosphate; PI(4)P, phosphatidylinositol 4-phosphate; PI(5)P, phosphatidylinositol 5-phosphate; PE, phosphatidylethanolamine; PC, phosphatidylcholine; S1P, sphingosine 1-phosphate; $PI(3,4)P_2$, phosphatidylinositol 3,4-bisphosphate; $PI(3,5)P_2$, phosphatidylinositol 3,5-bisphosphate; $PI(4,5)P_2$, phosphatidylinositol 4,5-bisphosphate; $PI(3,4,5)P_3$, phosphatidylinositol 3,4,5-trisphosphate; PA, phosphatidic acid; PS, phosphatidylserine; blue blank, lipid-negative control.

NaD1 or L5 but reached a similar plateau of fluorescence after 130 min. Initial permeabilization by L4A was at a rate similar to that of NaD1 and L5, but the fluorescence reached a plateau at a lower level. L1B and L4B displayed the slowest permeabilization kinetics, but L4B fluorescence plateaued at the same lower level as that of L4A, whereas L1B continued to permeabilize the plasma membrane and achieved the same plateau as NaD1, L5, and L1A.

**Lipid binding.** The specificity of lipid binding of the defensin chimeras was examined using lipid strips (Fig. 5). Consistent with the findings of previous studies, NaD1 interacted strongly with $PI(4,5)P_2$ and NaD2 interacted preferentially with phosphatidic acid (PA) (10, 15) The chimeras L1B and L6-L7 had a similar pattern of lipid binding to NaD1, whereas the pattern for L5 resembled that for NaD2 with a preference for PA. The chimeras L1A, L4A, and L4B bound to several lipids with no preference for PA or $PI(4,5)P_2$.

**Activity of the L1B chimera against other pathogenic fungi.** As mentioned above, replacement of the loop 1B sequence of NaD1 with the corresponding sequence from NaD2 led to a substantial increase in activity against *F. oxysporum* compared to that of the other chimeras and NaD1. The activity of L1B chimera was thus tested against a range of other fungi (Table 1). L1B was about 10 times more effective than NaD1 against *F. oxysporum* and was also more active against the other agriculturally relevant pathogens: *F. graminearum* and *C. graminicola*. L1B also inhibited the growth of the human pathogen *A. flavus* with an $IC_{50}$ of 3.5 μM, whereas NaD1 had no effect at concen-

**TABLE 1** $IC_{50}$s of L1B loop swap chimera and NaD1 against other pathogenic fungi

| Fungal species | $IC_{50}$ (μM) | |
|---|---|---|
| | NaD1 | L1B |
| *Fusarium oxysporum* | 1.5 ± 0.25 | 0.16 ± 0.04 |
| *Fusarium graminearum* | 0.4 ± 0.3 | 0.28 ± 0.03 |
| *Colletotrichum graminicola* | 4.4 ± 0.1 | 2.0 ± 0.4 |
| *Aspergillus flavus* 5310 | >10 | 3.5 ± 2.28 |
| *Aspergillus parasiticus* 4467 | 4.5 ± 0.27 | 3.7 ± 1.17 |
| *Aspergillus niger* 5181 | 2.1 ± 0.76 | 2.2 ± 1.22 |
| *Candida albicans* DAY185 | 2.0 ± 0.07 | 2.0 ± 0.16 |
| *Cryptococcus neoformans* H99 | 2.0 ± 0.15 | 1.6 ± 0.56 |
| *Cryptococcus gattii* WM276 | 1.5 ± 0.59 | 1.6 ± 0.37 |

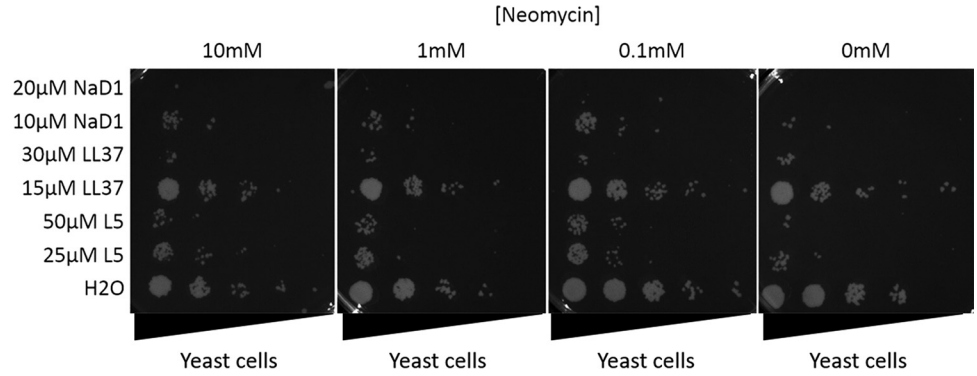


**FIG 6** Neomycin does not protect against the antifungal activity of NaD1, LL37, or L5. *S. cerevisiae* (BY4741) cells were treated with neomycin (0 to 10 mM) for 3 h, washed, and then treated with NaD1 (10 and 20 μM), LL37 (15 and 30 μM), or L5 (25 and 50 μM) for 1 h at 30°C. A 5-fold dilution series of each treatment was plated on YPD agar and grown at 30°C for 2 days. Neomycin did not protect against any of the antifungal peptides tested. Data are representative of those from three independent biological experiments.

trations up to 10 μM. This enhanced activity relative to that of NaD1 did not extend to the two other *Aspergillus* species tested. Similarly, the sensitivity of the yeast pathogens *C. albicans*, *C. neoformans*, and *Cryptococcus gattii* to L1B was unchanged compared to that to NaD1.

**Effect of PI(4,5)$P_2$ binding molecule neomycin on antifungal activity of NaD1.** Neomycin is an aminoglycoside antibiotic that binds to PI(4,5)$P_2$ (23) and blocks the antitumor activity of NaD1 and other defensins that bind to PI(4,5)$P_2$ (11, 17). To determine whether neomycin could block the antifungal activity of NaD1, we employed the model yeast *S. cerevisiae*, as the antifungal mechanism of action of NaD1 is conserved between filamentous fungi and yeast (21, 24). Yeast cells were treated with neomycin (0.1 to 10 mM), washed, and then treated with the antifungal peptides NaD1, L5, and LL37. LL37 was included as a non-PI(4,5)$P_2$ binding control. Survival was determined by plating serial dilutions of the treated yeast cells on YPD plates and assessing colony formation (Fig. 6A). Neomycin did not protect the yeast cells against the activity of any of the antifungal peptides.

**Activity of NaD1 against *S. cerevisiae* strains with deletions in genes that function in PI(4,5)$P_2$ biosynthesis.** The relationship between PI(4,5)$P_2$ binding and the antifungal activity of NaD1 was examined further using a series of *S. cerevisiae* strains that had deletions in the PI(4,5)$P_2$ biosynthetic machinery (Fig. 7C). Three of the deleted genes, *stt4*, *mss4*, and *pik1*, are essential to yeast viability; thus, the heterozygous diploid of each gene was assayed for changes in NaD1 sensitivity compared with that of wild-type diploid strain BY4743. The sensitivities of all other

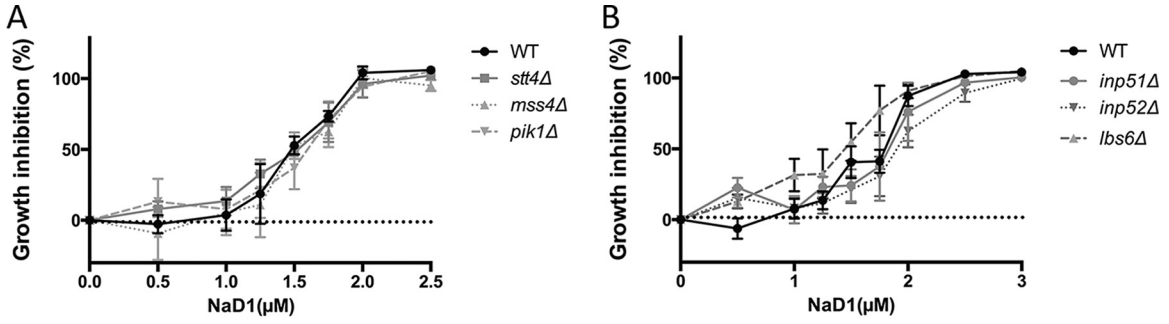


C

| Strain | Gene function | Effect on PI(4,5)$P_2$ |
|---|---|---|
| *STT4/stt4Δ* | Phosphatidylinositol-4-kinase [36] | Decreased [37] |
| *PIK1/pik1Δ* | Phosphatidylinositol 4-kinase [38] | Decreased [39] |
| *MSS4/mss4Δ* | Phosphatidylinositol-4-phosphate 5-kinase [40] | Decreased [40] |
| *Inp51Δ* | Phosphatidylinositol 4,5-bisphosphate 5-phosphatase [41] | Increased [41] |
| *Inp52Δ* | Polyphosphatidylinositol phosphatase [41] | Normal [41] |
| *lsb6Δ* | Type II phosphatidylinositol 4-kinase [42] | Normal [42] |

**FIG 7** Effect of NaD1 on the growth of *S. cerevisiae* mutants with gene knockouts in the PI(4,5)$P_2$ biosynthesis pathway. (A) The growth of *S. cerevisiae* cells with the heterozygous knockouts *pik1*Δ, *mss4*Δ, and *stt4*Δ was similar to the growth of the parent cell line BY4743 (wild type [WT]) in the presence of NaD1 (0 to 2.5 μM). (B) The growth inhibition of the *S. cerevisiae* nonessential PI(4,5)$P_2$ biosynthesis knockouts *lsb6*Δ, *inp51*Δ, and *inp52*Δ was similar to the growth inhibition of the parent cell line BY4741 (wild type) in the presence of NaD1 (0 to 3 μM). Growth was monitored by determination of the optical density at 595 nm over 24 h, and percent growth inhibition was plotted. Data are means ± SEMs ($n = 4$). (C) Functions of deleted genes and effects on PI(4,5)$P_2$ levels. The numbers in brackets represent reference citations (36–42).

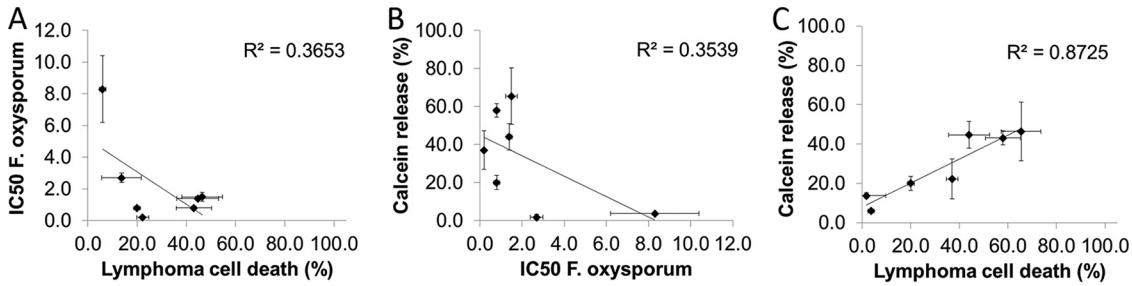


**FIG 8** Correlation of lymphoma cell death, calcein release from PI(4,5)$P_2$ liposomes, and $IC_{50}$ against *F. oxysporum*. Linear regression analysis was performed with the values for lymphoma death, calcein release, and $IC_{50}$ against *F. oxysporum* from Fig. 3. The $IC_{50}$ against *F. oxysporum* had $R^2$ values of 0.3653 and 0.3539 for lymphoma cell death and calcein release, respectively, indicating a poor correlation. Calcein release and lymphoma cell death had an $R^2$ value of 0.8725, indicating a strong correlation between the two values across the defensin chimeras.

strains were compared with the sensitivity of wild-type haploid strain BY4741. None of the deletion strains differed significantly in their sensitivity to NaD1 (Fig. 7A and B).

## DISCUSSION

The plant defensin NaD1 is produced in the flowers of the ornamental tobacco and functions to protect the reproductive tissues from damage by fungal pathogens (25). It also efficiently kills mammalian tumor cells at concentrations that have little effect on normal cells (10). We prepared chimeras of NaD1 and a second defensin, NaD2, that is produced in the same tissues as NaD1. NaD2 is not as potent an antifungal molecule as NaD1 and has no activity against tumor cells (Fig. 3). The overall aim of the work was to identify the features of NaD1 that are responsible for its potent activity against fungal and tumor cells with the objective of using this knowledge to generate more active and specific defensins for use in agriculture and medicine. These chimeras were prepared by replacing, in turn, each of the seven surface loops on NaD1 with the equivalent loops from NaD2. Apart from the chimeras with the loop 2 and 3 substitutions, all the loop swaps were tolerated and the proteins were expressed and correctly folded, allowing us to examine the relative importance of loops 1, 4, 5, 6, and 7 to the antifungal and tumor cell activity of NaD1. The longer loops, i.e., loops 1 and 4, were each divided into two sections, loops 1A and 1B and loops 4A and 4B, respectively, whereas shorter loops 6 and 7 were combined. Each of the loop swap chimeras was tested for activity against fungal (*F. oxysporum*) and tumor (U937) cells. The established role for PI(4,5)$P_2$ binding in tumor cell killing by NaD1 led to the investigation of the interaction between the loop swap variants and phospholipids, particularly PI(4,5)$P_2$.

Replacement of loop 1A, loop 1B, loop 4B, or loop 5 of NaD1 with the corresponding sequence of NaD2 decreased the activity against tumor cells compared to that of NaD1. Apart from L1B, each of these substitutions also had a major effect on PI(4,5)$P_2$ binding and permeabilization of PI(4,5)$P_2$ liposomes, consistent with previous reports (10, 11) that PI(4,5)$P_2$ binding and oligomerization of the defensin are crucial for the tumor cell killing activity of NaD1. The structure of NaD1 in complex with PI(4,5)$P_2$ revealed that 4 of the 6 residues from loop 5 (K36, L37, L38, and R40) form the primary lipid binding domain of NaD1 (10). Apart from R40, these residues are very different in NaD2, explaining why NaD2 and the NaD1 chimera with loop 5 from NaD2 do not bind to PI(4,5)$P_2$ on lipid strips and do not permeabilize PI(4,5)$P_2$-containing liposomes. The crystal structure also revealed that 3 of the 7 residues in loop 1A participate in the formation of the NaD1 dimer that is needed to produce the cationic grip structure that is essential for PI(4,5)$P_2$ binding. Of these three residues, R1, K4, and E6, the lysine at position 4 was the most crucial (10). Lay and colleagues reported that replacement of K4 with an alanine prevented dimer formation and increased the $IC_{50}$ 5-fold against fungal cells (26). The lysine at position 4 also participates in PI(4,5)$P_2$ binding. Consequently, both K4 (in loop 1A) and R40 (in loop 5) have been described to be the key residues involved in the formation of the oligomeric NaD1-PI(4,5)$P_2$ complex (10).

Another residue that interacts with PI(4,5)$P_2$ is H33 (10), which is 1 of the 4 residues in loop 4B. The chimera with the SGGD sequence from NaD2 in place of the TDGH loop 4B sequence of NaD1 had decreased activity compared with that of NaD1 against tumor cells, was less effective at permeabilizing PI(4,5)$P_2$ liposomes, and bound less well to PI(4,5)$P_2$ on lipid strips. These data support the role of H33 in the PI(4,5)$P_2$ interaction and the previously described role for D31 in the interaction between dimers required to form the oligomer (10). Replacement of the 5 residues in loop 4A of NaD1 (ISEKF) with the corresponding residues from NaD2 (LTEGF) had no significant effect on the activity of the chimera on tumor cells, fungal cells, or PI(4,5)$P_2$ liposomes, probably because the sequences are similar. Residue E27, which is required for dimer formation, is present in both.

The loop 6 and 7 substitution encompassed four residues: F42, which was changed to a leucine, and residues 44 to 46 (TKP), which were changed to TRP. K45 participates in dimer formation, but the conservative change to an arginine explains why the loop 6 and 7 substitution had no effect on activity against tumor cells, PI(4,5)$P_2$ binding, or liposome permeabilization.

There was a strong correlation between tumor cell killing activity and the level of permeabilization of PI(4,5)$P_2$ liposomes across the set of loop swap variants, further highlighting the importance of the NaD1-PI(4,5)$P_2$ interaction for the antitumor activity of NaD1 (Fig. 8). However, there was no correlation between antifungal activity and the permeabilization of PI(4,5)$P_2$ liposomes, indicating that PI(4,5)$P_2$ binding was not essential for the antifungal activity of all of the defensin chimeras. To further assess the role of PI(4,5)$P_2$ binding in the antifungal activity of NaD1, we determined whether neomycin has a protective effect in fungi similar to that observed with NaD1 and the tomato defensin TPP3 in tumor cells (10, 11). Neomycin did not protect yeast cells against

NaD1, LL37, or the L5 swap variant, confirming that $PI(4,5)P_2$ binding is not essential for the antifungal activity of NaD1, as it is for the antitumor activity. The lack of any significant difference in the sensitivity of yeast cells with gene deletions that cause changes in $PI(4,5)P_2$ levels and the sensitivity of yeast cells without gene deletions further supports the suggestion that the antifungal mechanism of NaD1 involves more than binding to $PI(4,5)P_2$. That is not to say that $PI(4,5)P_2$ binding does not have a role in antifungal activity but does suggest that other mechanisms must also be involved.

Many researchers have reported the importance of the loop 5 sequence for their antifungal defensins (reviewed in reference 27), and the high sequence variability in this region led to the hypothesis that they interact with different targets on fungal hyphae and, hence, have different mechanisms of action. Replacement of loop 5 and loss of $PI(4,5)P_2$ binding in the L5 chimera decreased the $IC_{50}$ against *F. oxysporum* by only 2-fold, but it abolished activity against tumor cells. Indeed, even though the L5 chimera failed to release calcein from the $PI(4,5)P_2$ liposomes, it was as effective as NaD1 in the permeabilization assays with *F. oxysporum* hyphae. That is, it was able to enter fungal cells and disrupt the plasma membrane in a $PI(4,5)P_2$-independent way. Considering the increased $IC_{50}$ for L5, it was surprising that L5 displayed permeabilization kinetics similar to those of NaD1. The permeabilization assay was conducted using protein concentrations in excess of the MIC and measures the rate of cell permeabilization by the peptide as opposed to the effect on fungal growth. Thus, the difference in observed $IC_{50}$s between NaD1 and L5 must be related to differences in the antifungal mechanism of these proteins that are not related to the rate of membrane permeabilization, such as a difference in affinity for a cell surface binding partner or ability to enter the cytoplasm. NaD2, the defensin from which the loop 5 sequence in the L5 chimera was taken, binds to PA and does not permeabilize the fungal membrane. Similarly, the $IC_{50}$ of L5 was more than 2-fold lower than that of NaD2, even though the two defensins have very similar lipid binding profiles on PIP strips. Hence, lipid binding is not the only determinant of antifungal activity and sequences other than loop 5 must be contributing to the improved activity of L5 compared to that of NaD2.

We hypothesize that NaD1 and, by extension, the loop swap chimeras have a three-step mechanism of action on fungal cells. The first interaction is with components of the fungal cell wall (13), which it traverses before coming into contact with the plasma membrane of fungal cells. It passes through the membrane by a mechanism that has not been defined, and once it reaches the cytoplasm it induces oxidative stress and permeabilizes the plasma membrane (13, 21). The reactive oxygen species (ROS) alone may be sufficient to initiate cell death. However, both ROS production and an interaction of NaD1 with $PI(4,5)P_2$ on the inner leaflet of the membrane would compromise the membrane and ensure that the cell cannot survive.

Knowing that $PI(4,5)P_2$ binding, dimerization, and oligomerization are all essential for the activity of NaD1 against tumor cells, we asked why NaD2 had no effect on tumor cells. NaD2 did not bind to $PI(4,5)P_2$ on the lipid strips or the $PI(4,5)P_2$-containing liposomes. This was expected because NaD2 lacks most of the amino acids that are crucial for $PI(4,5)P_2$ binding, and we have reported previously that it binds preferentially to PA (15).

As described for NaD1, loop 5 contains the residues that line the cationic grip and define the lipid binding specificity for the plant defensins. The loop 5 sequence of NaD2 is RGFRRR, which is present in several other antifungal plant defensins (7). One of these, MtDef4 from *Medicago truncatula*, has potent antifungal activity and has been well studied (28). It shares 85% sequence similarity with NaD2, and the loop 5 sequences are identical. Sagaram and colleagues (29) reported that, like NaD2, MtDef4 binds to PA. Furthermore, amino acid substitutions in loop 5 impair PA binding and abolish the ability of MtDef4 to enter and kill fungal cells. Thus, $PI(4,5)P_2$ binding is not required for the antifungal activity of all plant defensins. Indeed, $PI(4,5)P_2$ binding specificity has been reported only for type II defensins from the Solanaceae (15). Conversely, lipid binding alone is not sufficient for the antifungal activity of plant defensins. A single-amino-acid variant (Y38G) of RsAFP2 from radish bound to the cognate lipid glucosylceramide at levels similar to those of the wild-type defensin but had significantly impaired antifungal activity (30).

A common feature of antimicrobial peptides is that they carry a positive net charge to facilitate interactions with negatively charged microbial cell surfaces and the negatively charged lipid head groups in the plasma membrane (1). Tumor cells, like microbial cells, have an anionic plasma membrane outer leaflet (31) as well as a greater surface area and more fluid plasma membranes than normal cells (32). The activity of plant antimicrobial peptides against tumor cells could be the result of the increased susceptibility of tumor cells to cationic membrane-disrupting peptides, as they lack the protective capacity of a cell wall.

One of the most intriguing results from studies with the initial loop swap variants was the increased activity observed for L1B, L4A, and L6-L7 against *F. oxysporum*. NaD1 is more active as an antifungal molecule than NaD2. Thus, it was expected that replacement of the loop regions of NaD1 with those of NaD2 would be detrimental to antifungal activity, as was observed for antitumor activity. L1B was the most active of the loop swap variants, and although it retained $PI(4,5)P_2$ binding activity in the PIP strip assays, it displayed decreased permeabilization of $PI(4,5)P_2$ liposomes. Electrostatic interactions are a key component of the activity of cationic peptides, including defensins, against fungi (24), and L1B has an overall positive charge of +8, whereas that of NaD1 is +6 (Fig. 1) and that of NaD2 is +5. Modeling of the structure of the L1B chimera on the basis of the structure of NaD1 revealed that the two extra positively charged residues in loop 1B would not prevent the formation of the dimers that are required for antifungal activity (26), would not affect $PI(4,5)P_2$ binding, and are presented on the surface of the dimer (Fig. 9). The enhanced activity against fungal cells and decreased activity against tumor cells suggest that L1B interacts with a fungus-specific target and is not merely better at nonspecific disruption of negatively charged phospholipids in the plasma membrane. This is supported by the observation that L1B exhibited delayed permeabilization kinetics on fungal hyphae relative to those of NaD1 and was less active than NaD1 in the calcein release assay. Thus, it is likely that the enhanced activity of L1B is due an increased affinity for a target within the fungal cell wall or with an intracellular target that results in ROS production. L1B had enhanced activity against the filamentous fungi *F. graminearum*, *C. graminicola*, *A. flavus*, and, to a lesser extent, *A. parasiticus*. However, the activity of L1B against yeasts and *A. niger* was similar to that of NaD1. The observation that the enhancement in antifungal activity varied widely between fungal strains points to the potential involvement of the fungal cell wall, which varies between fungal species (33), and/or

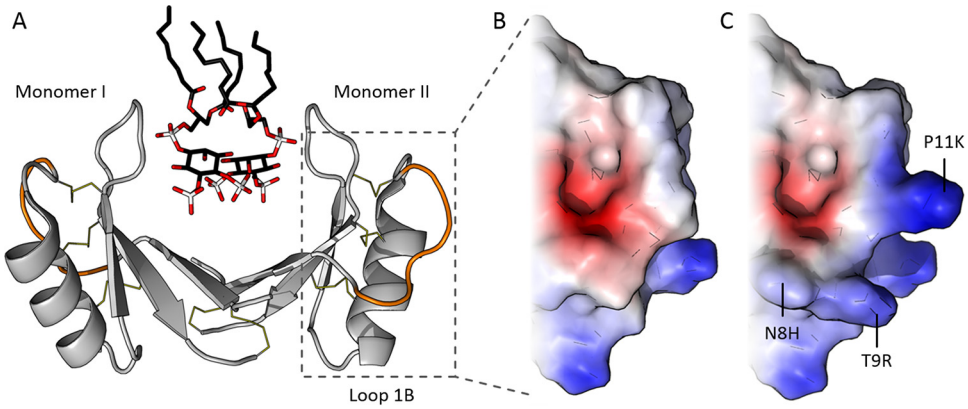


**FIG 9** Location of positively charged residues of L1B modeled onto the NaD1 structure. (A) Dimer of NaD1 with loop 1B highlighted in orange. $PI(4,5)P_2$ ligands are shown in black. (B) NaD1 surface potential with the positive charge in blue and the negative charge in red. (C) L1B surface charge with the mutations that increased the exposed positive charge indicated. The increase in positive charge is on the outer faces of the defensin dimer away from the $PI(4,5)P_2$ binding pocket. The structure was modified from the structure with PDB accession number 4CQK.

to differences in the ability of the fungi to respond to cell wall, osmotic, or oxidative stress (14, 21). Variations in cell wall composition have been proposed as an explanation for the different effects that the defensin MtDef4 displays against *Neurospora crassa* and *F. graminearum* (34).

Similar loop swap experiments have been conducted with human β-defensins to identify regions that produce the best antibacterial activity. Some chimeras had increased activity, whereas others were less active (35), leading to the proposal that sequence elements from different defensins make different contributions to antimicrobial activity. Analogously, the different loop regions in a plant defensin are likely to target different processes in the fungal cell, explaining why different defensins have different mechanisms of action. Swapping of loops between defensins could create new combinations of these functions in a single molecule. This has been proposed for dimers of short proline-rich antimicrobial peptides that are active against bacteria. Fusion of the DNA-K binding domain of pyrrhocoricin to the cell-penetrating region of drosocin increased activity against *E. coli* and allowed broader target specificity (30). In the context of NaD1, it remains to be determined whether loop 1B from NaD2 conferred new antifungal activity to the NaD1 backbone or enhanced the activity of the other loops of NaD1.

It remains to be elucidated whether the combination of the loop 1B sequence of NaD2 with other defensins would lead to an increase in antifungal activity and, conversely, whether loop 1B sequences from other class I defensins and/or other solanaceous class II defensin scaffolds could also be used to enhance or broaden the activity of antifungal plant defensins.

The constant threat from fungal pathogens has led plants to evolve an arsenal of innate immunity molecules for protection against devastating diseases. Plant defensins have a high degree of sequence variability outside the invariant cysteine residues that give them their characteristic structure. We propose that the loop regions between the cysteine cross-links have evolved as modular components that combine to form potent antifungal molecules. Artificial combinations of these loops can both enhance and diminish antifungal activity. The increase in antifungal activity obtained with some of these combinations suggests that nature has not yet developed the most potent antifungal plant defensin. Further shuffling of defensin sequences could produce antifungal peptides that are more active than those presented here and could lead to more desirable properties of this family of peptides for use in the treatment of fungal disease.

## ACKNOWLEDGMENTS

This work was supported by grants from ARC Discovery Projects to M.A.A., N.L.V.D.W., and M.D.H. (DP120102694) and M.A.A. and N.L.V.D.W. (DP150104386).

We thank Rosemary Guarino for her assistance with cloning, expression, and purification of the loop swap proteins.

## FUNDING INFORMATION

This work, including the efforts of Mark D. Hulett, Nicole L. van der Weerden, and Marilyn A. Anderson, was funded by Australian Research Council (ARC) (DP120102694). This work, including the efforts of Nicole L. van der Weerden and Marilyn A. Anderson, was funded by Australian Research Council (ARC) (DP150104386).

The funders had no role in study design, data collection and interpretation, or the decision to submit the work for publication.

## REFERENCES

1. **van der Weerden NL, Bleackley MR, Anderson MA.** 2013. Properties and mechanisms of action of naturally occurring antifungal peptides. Cell Mol Life Sci **70:**3545–3570 . http://dx.doi.org/10.1007/s00018-013-1260-1.
2. **Knogge W.** 1996. Fungal infection of plants. Plant Cell **8:**1711. http://dx.doi.org/10.1105/tpc.8.10.1711.
3. **Fisher MC, Henk DA, Briggs CJ, Brownstein JS, Madoff LC, McCraw SL, Gurr SJ.** 2012. Emerging fungal threats to animal, plant and ecosystem health. Nature **484:**186–194. http://dx.doi.org/10.1038/nature10947.
4. **De Coninck B, Cammue BPA, Thevissen K.** 2013. Modes of antifungal action and in planta functions of plant defensins and defensin-like peptides. Fungal Biol Rev **26:**109–120. http://dx.doi.org/10.1016/j.fbr.2012.10.002.
5. **van der Weerden NL, Anderson MA.** 2013. Plant defensins: common fold, multiple functions. Fungal Biol Rev **26:**121–131. http://dx.doi.org/10.1016/j.fbr.2012.08.004.
6. **Gaspar YM, McKenna JA, McGinness BS, Hinch J, Poon S, Connelly AA, Anderson MA, Heath RL.** 2014. Field resistance to Fusarium oxysporum and Verticillium dahliae in transgenic cotton expressing the plant defensin NaD1. J Exp Bot **65:**1541–1550. http://dx.doi.org/10.1093/jxb/eru021.
7. **Kaur J, Thokala M, Robert-Seilaniantz A, Zhao P, Peyret H, Berg H, Pandey S, Jones J, Shah D.** 2012. Subcellular targeting of an evolution-

arily conserved plant defensin MtDef4.2 determines the outcome of plant-pathogen interaction in transgenic Arabidopsis. Mol Plant Pathol **13:** 1032–1046. http://dx.doi.org/10.1111/j.1364-3703.2012.00813.x.

8. **Jha S, Chattoo BB.** 2010. Expression of a plant defensin in rice confers resistance to fungal phytopathogens. Transgenic Res **19:**373–384. http://dx.doi.org/10.1007/s11248-009-9315-7.
9. **Lay FT, Anderson MA.** 2005. Defensins—components of the innate immune system in plants. Curr Protein Pept Sci **6:**85–101. http://dx.doi.org/10.2174/1389203053027575.
10. **Poon I, Baxter AA, Lay FT, Mills GD, Adda CG, Payne JA, Phan TK, Ryan GF, White JA, Veneer PK, van der Weerden NL, Anderson MA, Kvansakul M, Hulett MD.** 2014. Phosphoinositide-mediated oligomerization of a defensin induces cell lysis. eLife **3:**e01808. http://dx.doi.org/10.7554/eLife.01808.
11. **Baxter AA, Richter V, Lay FT, Poon IK, Adda CG, Veneer PK, Phan TK, Bleackley MR, Anderson MA, Kvansakul M.** 2015. The tomato defensin TPP3 binds phosphatidylinositol (4,5)-bisphosphate via a conserved dimeric cationic grip conformation to mediate cell lysis. Mol Cell Biol **35:** 1964–1978. http://dx.doi.org/10.1128/MCB.00282-15.
12. **van der Weerden NL, Lay FT, Anderson MA.** 2008. The plant defensin, NaD1, enters the cytoplasm of Fusarium oxysporum hyphae. J Biol Chem **283:**14445–14452. http://dx.doi.org/10.1074/jbc.M709867200.
13. **van der Weerden NL, Hancock RE, Anderson MA.** 2010. Permeabilization of fungal hyphae by the plant defensin NaD1 occurs through a cell wall-dependent process. J Biol Chem **285:**37513–37520. http://dx.doi.org/10.1074/jbc.M110.134882.
14. **Hayes BM, Anderson MA, Traven A, van der Weerden NL, Bleackley MR.** 2014. Activation of stress signalling pathways enhances tolerance of fungi to chemical fungicides and antifungal proteins. Cell Mol Life Sci **71:**2651–2666. http://dx.doi.org/10.1007/s00018-014-1573-8.
15. **Payne JA, Bleackley MR, Lee T-H, Shafee TM, Poon IK, Hulett MD, Aguilar M-I, van der Weerden NL, Anderson MA.** 2016. The plant defensin NaD1 introduces membrane disorder through a specific interaction with the lipid, phosphatidylinositol 4,5 bisphosphate. Biochim Biophys Acta **1858:**1099–1109. http://dx.doi.org/10.1016/j.bbamem.2016.02.016.
16. **Shafee TM, Lay FT, Hulett MD, Anderson MA.** 13 June 2016. The defensins consist of two independent, convergent protein superfamilies. Mol Biol Evol Epub ahead of print.
17. **Phan TK, Lay FT, Poon I, Hinds MG, Kvansakul M, Hulett MD.** 2016. Human β-defensin 3 contains an oncolytic motif that binds PI(4,5)P2 to mediate tumour cell permeabilisation. Oncotarget **7:**2054–2069. http://dx.doi.org/10.18632/oncotarget.6520.
18. **Dracatos PM, Weerden NL, Carroll KT, Johnson ED, Plummer KM, Anderson MA.** 2014. Inhibition of cereal rust fungi by both class I and II defensins derived from the flowers of Nicotiana alata. Mol Plant Pathol **15:**67–79. http://dx.doi.org/10.1111/mpp.12066.
19. **Catanzariti AM, Soboleva TA, Jans DA, Board PG, Baker RT.** 2004. An efficient system for high-level expression and easy purification of authentic recombinant proteins. Protein Sci **13:**1331–1339. http://dx.doi.org/10.1110/ps.04618904.
20. **de Araujo AD, Hoang HN, Kok WM, Diness F, Gupta P, Hill TA, Driver RW, Price DA, Liras S, Fairlie DP.** 2014. Comparative α-helicity of cyclic pentapeptides in water. Angew Chem Int Ed Engl **53:**6965–6969. http://dx.doi.org/10.1002/anie.201310245.
21. **Hayes BM, Bleackley MR, Wiltshire JL, Anderson MA, Traven A, van der Weerden NL.** 2013. Identification and mechanism of action of the plant defensin NaD1 as a new member of the antifungal drug arsenal against Candida albicans. Antimicrob Agents Chemother **57:**3667–3675. http://dx.doi.org/10.1128/AAC.00365-13.
22. **Zhang L, Rozek A, Hancock RE.** 2001. Interaction of cationic antimicrobial peptides with model membranes. J Biol Chem **276:**35714–35722. http://dx.doi.org/10.1074/jbc.M104925200.
23. **Gabev E, Kasianowicz J, Abbott T, McLaughlin S.** 1989. Binding of neomycin to phosphatidylinositol 4,5-biphosphate (PIP 2). Biochim Biophys Acta **979:**105–112. http://dx.doi.org/10.1016/0005-2736(89)90529-4.
24. **Bleackley MR, Wiltshire JL, Perrine-Walker F, Vasa S, Burns RL, van der Weerden NL, Anderson MA.** 2014. The plasma membrane transregulator of polyamine uptake Agp2p regulates the antifungal activity of the plant defensin NaD1 and other cationic peptides. Antimicrob Agents Chemother **58:**2688–2698. http://dx.doi.org/10.1128/AAC.02087-13.
25. **Lay FT, Brugliera F, Anderson MA.** 2003. Isolation and properties of floral defensins from ornamental tobacco and petunia. Plant Physiol **131:** 1283–1293. http://dx.doi.org/10.1104/pp.102.016626.
26. **Lay FT, Mills GD, Poon IK, Cowieson NP, Kirby N, Baxter AA, van der Weerden NL, Dogovski C, Perugini MA, Anderson MA, Kvansakul M, Hulett MD.** 2012. Dimerization of plant defensin NaD1 enhances its antifungal activity. J Biol Chem **287:**19961–19972. http://dx.doi.org/10.1074/jbc.M111.331009.
27. **Lacerda AF, Vasconcelos ÉA, Pelegrini PB, Grossi de Sa MF.** 2014. Antifungal defensins and their role in plant defense. Front Microbiol **5:**116. http://dx.doi.org/10.3389/fmicb.2014.00116.
28. **Sagaram US, Pandurangi R, Kaur J, Smith TJ, Shah DM.** 2011. Structure-activity determinants in antifungal plant defensins MsDef1 and MtDef4 with different modes of action against Fusarium graminearum. PLoS One **6:**e18550. http://dx.doi.org/10.1371/journal.pone.0018550.
29. **Sagaram US, El-Mounadi K, Buchko GW, Berg HR, Kaur J, Pandurangi RS, Smith TJ, Shah DM.** 2013. Structural and functional studies of a phosphatidic acid-binding antifungal plant defensin MtDef4: identification of an RGFRRR motif governing fungal cell entry. PLoS One **8:**e82485. http://dx.doi.org/10.1371/journal.pone.0082485.
30. **Thevissen K, Warnecke DC, François IE, Leipelt M, Heinz E, Ott C, Zähringer U, Thomma BP, Ferket KK, Cammue BP.** 2004. Defensins from insects and plants interact with fungal glucosylceramides. J Biol Chem **279:**3900–3905.
31. **Abercrombie M, Ambrose E.** 1962. The surface properties of cancer cells: a review. Cancer Res **22**(5 Part 1)**:**525–548.
32. **Sok M, Šentjurc M, Schara M.** 1999. Membrane fluidity characteristics of human lung cancer. Cancer Lett **139:**215–220. http://dx.doi.org/10.1016/S0304-3835(99)00044-0.
33. **Mélida H, Sain D, Stajich JE, Bulone V.** 2015. Deciphering the uniqueness of Mucoromycotina cell walls by combining biochemical and phylogenomic approaches. Environ Microbiol **17:**1649–1662. http://dx.doi.org/10.1111/1462-2920.12601.
34. **El-Mounadi K, Islam KT, Hernández-Ortiz P, Read ND, Shah DM.** 2016. Antifungal mechanisms of a plant defensin MtDef4 are not conserved between the ascomycete fungi Neurospora crassa and Fusarium graminearum. Mol Microbiol **100:**542–559. http://dx.doi.org/10.1111/mmi.13333.
35. **Jung S, Mysliwy J, Spudy B, Lorenzen I, Reiss K, Gelhaus C, Podschun R, Leippe M, Grötzinger J.** 2011. Human β-defensin 2 and β-defensin 3 chimeric peptides reveal the structural basis of the pathogen specificity of their parent molecules. Antimicrob Agents Chemother **55:**954–960. http://dx.doi.org/10.1128/AAC.00872-10.
36. **Audhya A, Emr SD.** 2002. Stt4 PI 4-kinase localizes to the plasma membrane and functions in the Pkc1-mediated MAP kinase cascade. Dev Cell **2:**593–605. http://dx.doi.org/10.1016/S1534-5807(02)00168-5.
37. **Perera NM, Michell RH, Dove SK.** 2004. Hypo-osmotic stress activates Plc1p-dependent phosphatidylinositol 4,5-bisphosphate hydrolysis and inositol hexakisphosphate accumulation in yeast. J Biol Chem **279:**5216–5226. http://dx.doi.org/10.1074/jbc.M305068200.
38. **Flanagan CA, Schnieders EA, Emerick AW, Kunisawa R, Admon A, Thorner J.** 1993. Phosphatidylinositol 4-kinase: gene structure and requirement for yeast cell viability. Science **262:**1444–1448. http://dx.doi.org/10.1126/science.8248783.
39. **Audhya A, Foti M, Emr SD.** 2000. Distinct roles for the yeast phosphatidylinositol 4-kinases, Stt4p and Pik1p, in secretion, cell growth, and organelle membrane dynamics. Mol Biol Cell **11:**2673–2689. http://dx.doi.org/10.1091/mbc.11.8.2673.
40. **Desrivières S, Cooke FT, Parker PJ, Hall MN.** 1998. MSS4, a phosphatidylinositol-4-phosphate 5-kinase required for organization of the actin cytoskeleton in Saccharomyces cerevisiae. J Biol Chem **273:**15787–15793. http://dx.doi.org/10.1074/jbc.273.25.15787.
41. **Stolz LEC, Huynh V, Thorner J, York JD.** 1998. Identification and characterization of an essential family of inositol polyphosphate 5-phosphatases (INP51, INP52 and INP53 gene products) in the yeast Saccharomyces cerevisiae. Genetics **148:**1715–1729.
42. **Han G-S, Audhya A, Markley DJ, Emr SD, Carman GM.** 2002. The Saccharomyces cerevisiae LSB6 gene encodes phosphatidylinositol 4-kinase activity. J Biol Chem **277:**47709–47718. http://dx.doi.org/10.1074/jbc.M207996200.